http://dx.doi.org/10.2106/jbjs.18.00867

The following content was supplied by the authors as supporting material and has not been copy-edited or verified by JBJS.

Appendix A: Specimen Evaluation and Robotic Gait Simulator (RGS) Validation

Ten fresh-frozen cadaveric right-lower-limb specimens were initially obtained for experimentation. One specimen failed during gait simulation due to bilateral malleolar fractures and dislocation of prosthetic talar component; this specimen's data was excluded from the study. Another specimen completed gait simulations for all conditions except 9A due to failure of the talar component's PMMA fixation; the specimen's data collected prior to failure were included in the study. The remaining eight specimens completed gait simulations for all conditions.

The RGS accurately replicated the target vGRF and tibia-to-ground kinematics previously collected from six subjects who received a Salto Talaris® Total Ankle Prosthesis one year prior to data collection. Each subject performed five gait trials in our motion analysis laboratory. A twelve-camera motion analysis system (Vicon; Lake Forest, CA) sampling at 120 Hz recorded tibia motion and a force plate (Kistler Instrument Corp., Amherst, NY) sampling at 1200 Hz recorded the vGRF. The 30 trials were then averaged. In vitro vGRF root mean square (RMS) error from the target data averaged 5.5% body weight; the greatest deviations from target vGRF values occurred within the first and last 10% of stance phase (**Figure A1**). The RGS successfully reproduced target tibia-to-ground kinematics within one standard deviation of the target data (**Figure A2**). The RGS also closely tracked prescribed muscle forces; the average RMS error for tendons was 3.0 N excluding the Achilles and tibialis anterior tendons, which were under fuzzy logic control (**Figure A3**).

http://dx.doi.org/10.2106/jbjs.18.00867

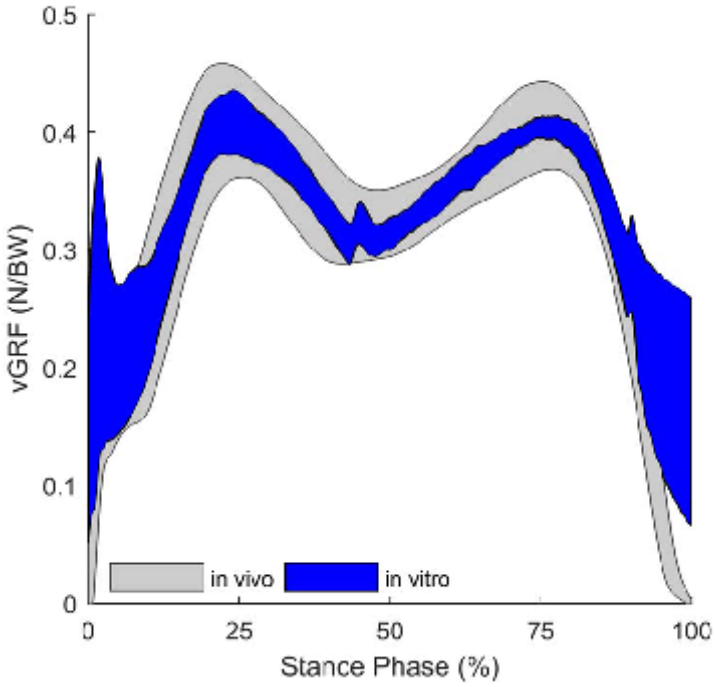

Figure A1: Vertical ground reaction force (vGRF) validation. Mean ± 1 standard deviation (SD) in vitro vGRF produced by the robotic gait simulator (RGS) compared to in vivo target vGRF ± 1 SD collected from one-year postoperative total ankle arthroplasty subjects.

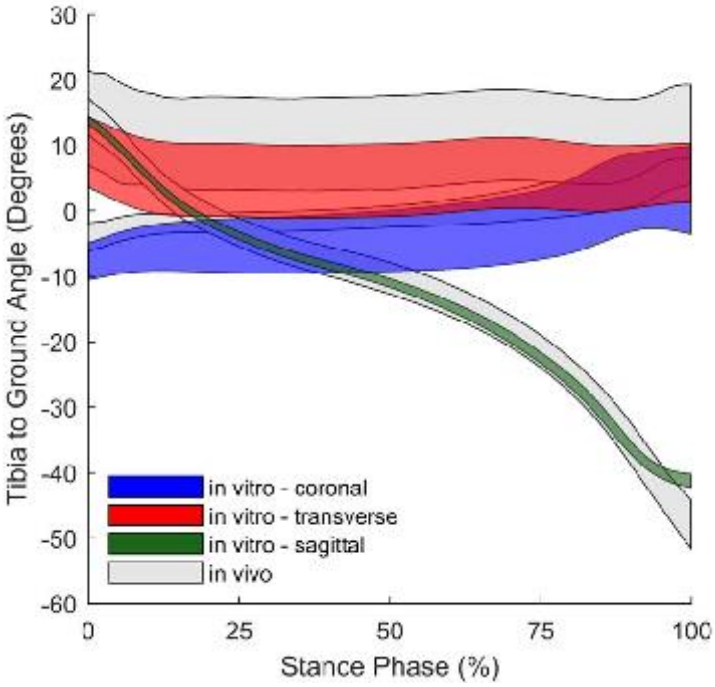

Figure A2: Tibia-to-ground kinematic validation. Mean ± 1 SD for in vitro tibia-to-ground kinematics produced by the robotic gait simulator (RGS) in the coronal, transverse, and sagittal planes for all specimens compared to in vivo mean kinematics ± 1 SD collected from one-year postoperative total ankle arthroplasty subjects.

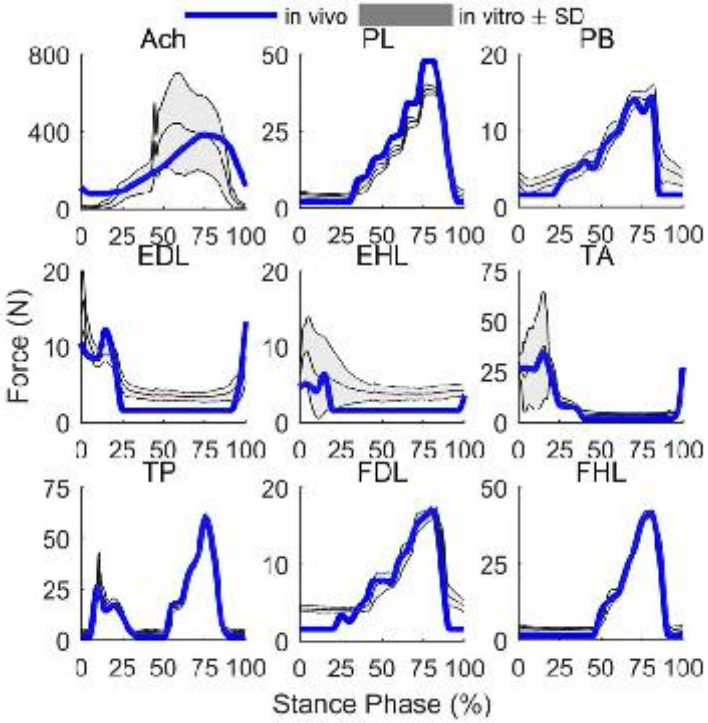

Figure A3: Estimated in vivo target tendon forces and mean ± 1 SD in vitro tendon forces for all specimens. In vitro tendon forces for the Achilles and tibialis anterior do not follow target forces as they are altered by the fuzzy logic controller. Ach = Achilles, PL = peroneus longus, PB = peroneus brevis, EDL = extensor digitorum longus, EHL = extensor hallucis longus, TA = tibialis anterior, TP = tibialis posterior, FDL = flexor digitorum longus, FHL = flexor hallucis longus.

Appendix B: Mean Range of Motion and Statistically Significant Changes in Stance Phase Interval with Associated Changes in Joint Position

Table B1 shows the mean range of motion ± SE by condition for all joints and bone-to-bone relationships observed within this study. Select joints were included in the manuscript to demonstrate significant trends. Table B2 shows statistically significant changes in stance phase interval for all joints and bone-to-bone relationships, for all alignment conditions with associated changes in joint position; comparisons for alignment conditions and joint position were made relative to the neutral (N) alignment.

Table 1: Mean Range of Motion ± SE by Condition (Degrees)

Joint or Relationship	Cardinal Plane	9A	6A	3A	N	3P	6P	9P	Omnibus *p*-value
Tibiotalar	Coronal	2.4 ± 0.6	2.5 ± 0.5	2.4 ± 0.5	2.7 ± 0.5	2.8 ± 0.6	2.6 ± 0.6	3.1 ± 0.7	0.22
	Transverse	3.0 ± 0.6	2.5 ± 0.5	2.7 ± 0.5	2.6 ± 0.5	3.7 ± 0.7	4.0 ± 0.7*	4.9 ± 0.7**	<0.0005†
	Sagittal	15.9 ± 0.8	15.9 ± 0.7*	15.8 ± 0.7	15.3 ± 0.7	13.5 ± 0.7**	11.4 ± 0.9**	11.8 ± 1.0**	<0.0005†
Talocalcaneal	Coronal	4.5 ± 0.7	4.6 ± 0.6	4.2 ± 0.5	3.7 ± 0.4	3.8 ± 0.4	3.9 ± 0.4	3.5 ± 0.5	0.134
	Transverse	4.1 ± 0.5	4.2 ± 0.5	3.8 ± 0.5	3.8 ± 0.4	4.4 ± 0.5	4.7 ± 0.6	4.0 ± 0.5	0.092
	Sagittal	4.1 ± 0.5	4.2 ± 0.5	3.8 ± 0.5	3.8 ± 0.4	4.4 ± 0.5	4.7 ± 0.6	4.0 ± 0.5	0.093
Talonavicular	Coronal	8.2 ± 1.3	8.2 ± 1.1	7.3 ± 1.1	7.4 ± 1.1	7.6 ± 1.1	7.9 ± 1.1	7.9 ± 1.2	0.10
	Transverse	7.8 ± 1.1	7.8 ± 1.1	8.0 ± 1.1	8.3 ± 1.1	9.1 ± 1.1	9.5 ± 1.2	8.4 ± 1.4	0.052
	Sagittal	6.4 ± 0.7	6.2 ± 0.8	6.4 ± 0.7*	7.0 ± 0.7	7.7 ± 0.8	8.4 ± 1.2	7.0 ± 1.3	0.0006†
Calcaneocuboid	Coronal	4.0 ± 0.8	3.1 ± 0.7	3.2 ± 0.6	3.5 ± 0.5	3.9 ± 0.5	3.8 ± 0.6	3.7 ± 0.6	0.47
	Transverse	4.4 ± 0.6	4.5 ± 0.9	4.3 ± 0.8	4.1 ± 0.6	4.0 ± 0.7	5.8 ± 0.9	6.4 ± 0.8**	0.012†
	Sagittal	4.6 ± 1.0	4.3 ± 0.8*	5.5 ± 0.7	5.6 ± 0.6	6.3 ± 0.7*	7.3 ± 0.7**	7.6 ± 0.7**	<0.0005†
Naviculocuneiform	Coronal	6.2 ± 0.5*	6.6 ± 0.5	6.5 ± 0.6	6.6 ± 0.5	6.3 ± 0.6	6.3 ± 0.6	5.6 ± 0.7	0.01†
	Transverse	5.1 ± 1.3	5.4 ± 1.3	5.5 ± 1.3	5.6 ± 1.3	5.8 ± 1.3	5.8 ± 1.3	5.2 ± 1.1	0.47
	Sagittal	9.3 ± 1.3	9.5 ± 1.3	9.6 ± 1.2	9.3 ± 1.2	8.9 ± 1.2	8.7 ± 1.3	8.7 ± 1.3	0.20
First Tarsometatarsal	Coronal	6.5 ± 1.3	6.8 ± 1.3	5.4 ± 1.3	5.9 ± 1.2	6.3 ± 1.2	5.8 ± 1.2	5.3 ± 1.3	0.24
	Transverse	4.2 ± 0.9	4.7 ± 0.9	4.2 ± 0.8	4.4 ± 0.7	4.8 ± 0.8	4.5 ± 0.8	4.7 ± 0.9	0.66
	Sagittal	3.3 ± 0.5	3.3 ± 0.5	3.4 ± 0.4	3.6 ± 0.3	3.7 ± 0.4	3.2 ± 0.4**	3.4 ± 0.4	0.039†
First Metatarsal to Tibia	Coronal	8.2 ± 1.4	7.4 ± 1.0	6.3 ± 0.9	6.6 ± 0.8	6.5 ± 0.9	6.3 ± 1.0	5.8 ± 1.1	0.47
	Transverse	8.0 ± 1.0	8.6 ± 0.8	8.3 ± 0.8	8.3 ± 0.7	8.1 ± 0.8	8.0 ± 1.0	8.6 ± 0.9	0.97
	Sagittal	25.8 ± 0.8	25.5 ± 0.7	25.4 ± 0.7	25.0 ± 0.6	24.1 ± 0.8	21.7 ± 1.5	19.9 ± 1.6**	0.0003†
First Metatarsal to Talus	Coronal	8.6 ± 1.6	7.6 ± 1.0	6.6 ± 0.9	6.7 ± 0.8	6.4 ± 0.9	5.9 ± 1.0	6.0 ± 1.0	0.33
	Transverse	7.8 ± 1.1*	9.0 ± 1.1	8.5 ± 1.0	9.4 ± 0.9	10.1 ± 1.1	10.1 ± 1.1	9.9 ± 1.2	0.03†
	Sagittal	14.8 ± 0.9	15.1 ± 0.8	15.4 ± 0.7	15.6 ± 0.7	16.3 ± 0.8	16.0 ± 1.1	14.8 ± 1.2	0.26

First Metatarsophalangeal	Coronal	20.9 ± 3.1	21.2 ± 2.9	21.7 ± 2.7	20.8 ± 2.7	23.4 ± 3.3	18.9 ± 3.0	18.4 ± 3.7	0.364
	Transverse	22.8 ± 2.9	24.0 ± 2.8	23.4 ± 2.7	22.3 ± 2.7	24.2 ± 3.6	19.8 ± 2.9	21.1 ± 3.4	0.013†
	Sagittal	50.5 ± 2.0	50.4 ± 2.1	50.5 ± 2.1	48.6 ± 1.9	47.5 ± 3.0	42.5 ± 2.1**	40.9 ± 3.3*	<0.0005†
Fifth Tarsometatarsal	Coronal	7.0 ± 1.0	6.4 ± 1.0	6.7 ± 0.9	6.6 ± 0.8	6.3 ± 1.0	6.1 ± 1.1	6.4 ± 0.9	0.93
	Transverse	12.6 ± 2.1	11.2 ± 1.6	10.1 ± 1.5	9.6 ± 1.4	10.9 ± 1.5	12.3 ± 1.9	13.6 ± 2.4	0.012†
	Sagittal	16.8 ± 3.6	16.3 ± 2.7	14.1 ± 2.5	14.6 ± 2.3	15.7 ± 2.4	17.7 ± 2.9	18.8 ± 2.9	0.0282†

†Significance of the omnibus test for association between outcome for all conditions. Pairwise comparisons were made between range of motion of the N alignment and all other alignment conditions. *Pairwise differences with $p < 0.05$. **Pairwise differences with $p < 0.005$. A = anterior, N = neutral, P = posterior. SE = standard error.

Table 2: Statistically Significant Stance Phase Interval (%) Compared to N and Associated Change in Joint Position.

Joint or Relationship	9A	6A	3A	3P	6P	9P
Tibiotalar	• 0-28, 76-100 plantar flexion • 0-100 inversion	• 0-31, 34-100 plantar flexion • 0-100 inversion	• 0-100 plantar flexion • 54-100 inversion	• 0-23, 94-100 dorsiflexion • 0-59, 93-100 eversion	• 0-100 dorsiflexion • 0-69, 91-100 eversion	• 0-100 dorsiflexion • 0-100 eversion
Talocalcaneal	• 21-26, 69-92 eversion • 15-58, 86-96 abduction	• 58-71 dorsiflexion • 44-55, 65-81 eversion • 22-37, 66-80 abduction	• 17-31, 46-66 dorsiflexion • 25-100 eversion • 17-100 abduction	• 0-62, 76-95 plantar flexion • 1-7, 26-34, 61-69 inversion • 0-100 adduction	• 0-100 plantar flexion • 0-100 inversion • 0-100 adduction	• 0-100 plantar flexion • 0-100 inversion • 0-100 adduction
Talonavicular	• 0-4, 13-21 dorsiflexion • 0-100 abduction	• 0-22, 65-74, 86-94 dorsiflexion • 6-44 abduction	• 7-100 eversion • 0-100 abduction	• 0-54, 72-82, 87-99 plantar flexion • 6-18 inversion • 0-28 adduction	• 0-99 plantar flexion • 0-100 inversion • 0-100 adduction	• 0-100 plantar flexion • 0-100 inversion • 0-100 adduction
Naviculocuneiform	—	—	—	—	• 13-19 plantar flexion	• 13-19 plantar flexion
Calcaneocuboid	• 3-11 dorsiflexion	• 2-40 dorsiflexion • 82-92 adduction	• 35-43 adduction	• 8-16 plantar flexion	• 6-18 plantar flexion	• 11-16, 33-42 plantar flexion
First Tarsometatarsal	—	—	—	—	—	—
First Metatarsal to Tibia	• 0-7, 87-100 plantar flexion	• 0-8, 69-100 plantar flexion	• 0-5 plantar flexion • 63-77 eversion	• 93-97 inversion	• 0-8 dorsiflexion • 5-25 inversion • 7-100 adduction	• 0-6 dorsiflexion • 15-47,79-96 inversion • 0-100 adduction

First Metatarsal to Talus	• 83-88 eversion	• 7-23 dorsiflexion • 33-37, 74-80 eversion	• 63-87 eversion	• 0-37 plantar flexion • 2-14, 37-60, 89-100 inversion • 0-20, 95-100 adduction	• 0-95 plantar flexion • 0-28, 38-100 inversion • 0-100 adduction	• 0-100 plantar flexion • 0-100 inversion • 0-100 adduction
Fifth Tarsometatarsal	—	—	• 51-86 plantar flexion	• 10-14 plantar flexion	—	• 11-18 plantar flexion • 62-66, 78-88 dorsiflexion
First Metatarsophalangeal	—	• 8-16 plantar flexion • 71-86, 91-100 dorsiflexion • 93-97 abduction	• 92-100 dorsiflexion	• 9-33 dorsiflexion	• 10-57 dorsiflexion • 8-41 abduction	• 11-55 dorsiflexion • 24-40 abduction

A = anterior, N = neutral, P = posterior.

http://dx.doi.org/10.2106/jbjs.18.00867

Appendix C: All Joint Kinematics

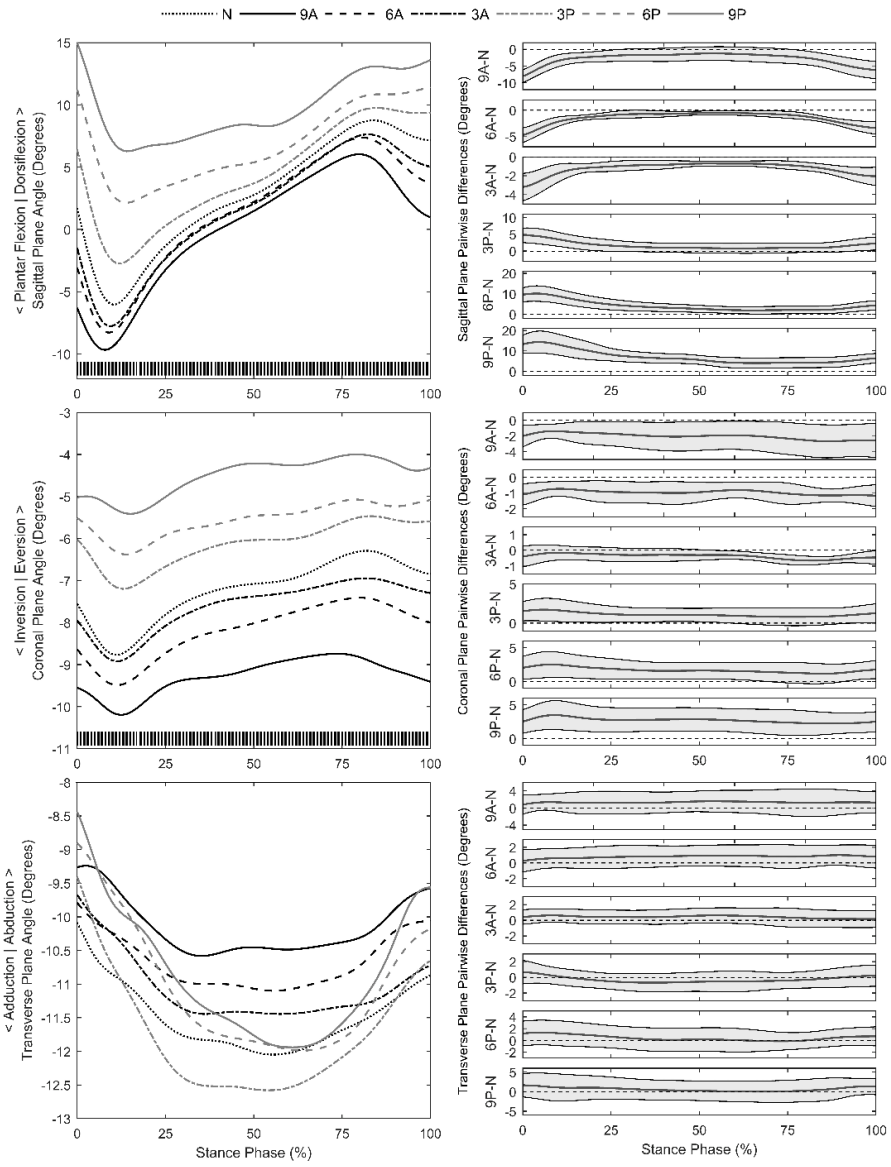

Figure C1: Left column) Mean tibiotalar joint kinematics in the sagittal, coronal, and transverse planes during stance phase for all specimens. Significant omnibus differences between mean joint angles are depicted by tick marks along the x-axis. Right column) Pairwise differences between each malalignment and the N alignment. Significance occurs when zero lies outside the 95% confidence interval. Tibiotalar joint kinematics reflect motion of the talus with respect to the tibia.

http://dx.doi.org/10.2106/jbjs.18.00867

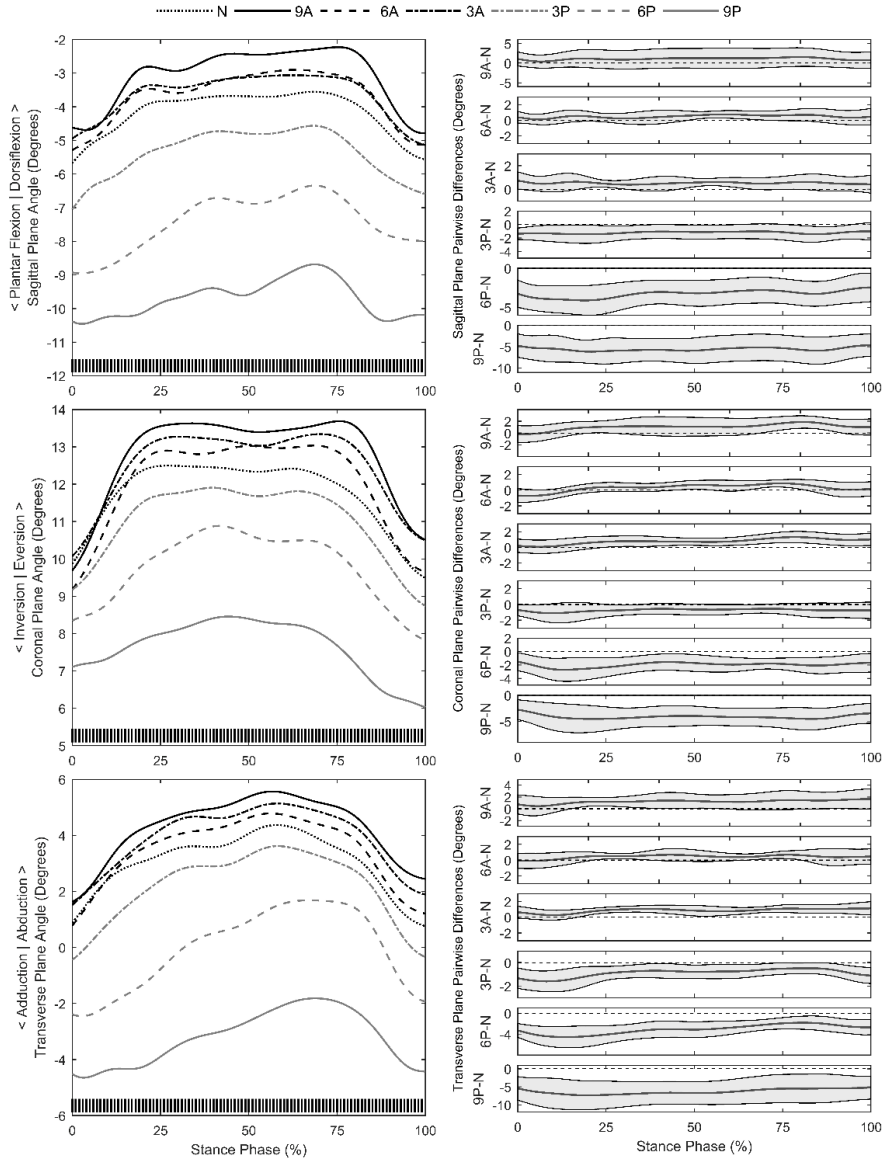

Figure C2: Left column) Mean talocalcaneal joint kinematics in the sagittal, coronal, and transverse planes during stance phase for all specimens. Significant omnibus differences between mean joint angles are depicted by tick marks along the x-axis. Right column) Pairwise differences between each malalignment and the N alignment. Significance occurs when zero lies outside the 95% confidence interval. Talocalcaneal joint kinematics reflect motion of the calcaneus with respect to the talus.

http://dx.doi.org/10.2106/jbjs.18.00867

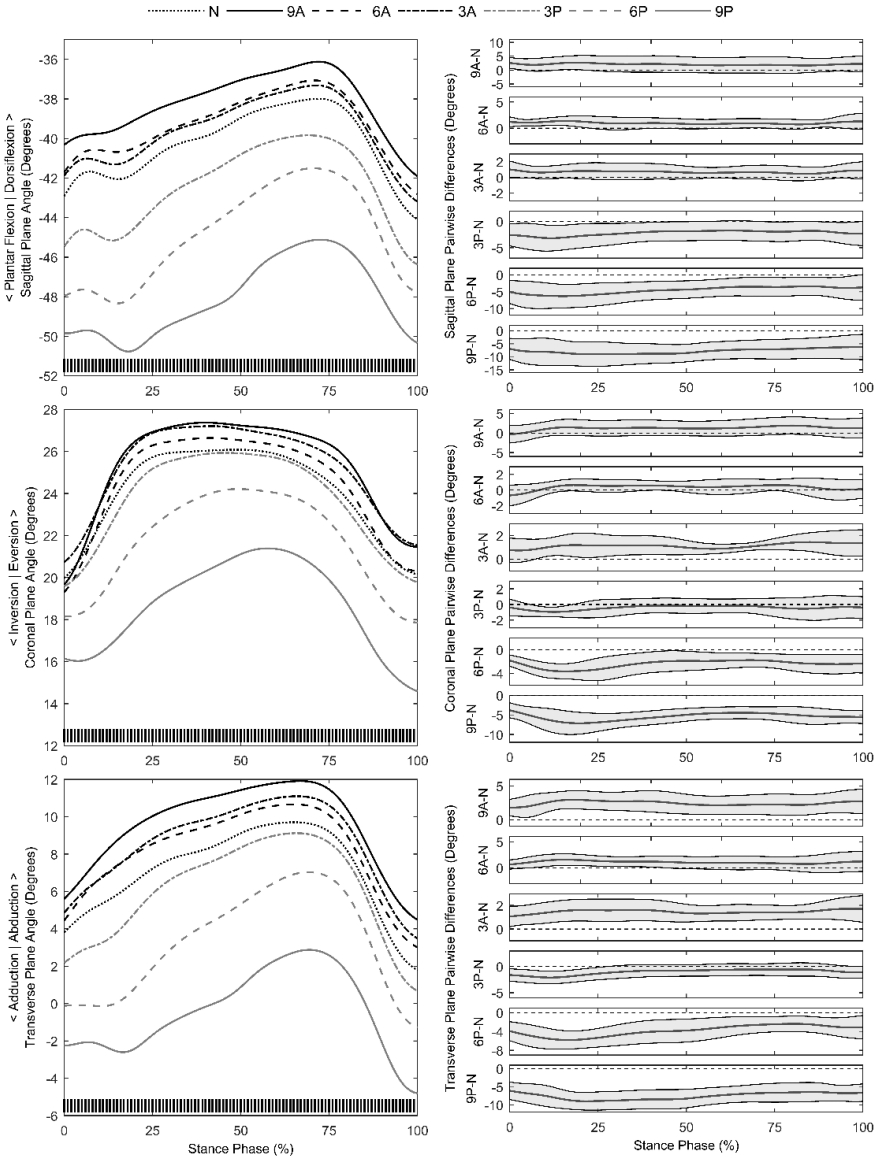

Figure C3: Left column) Mean calcaneocuboid joint kinematics in the sagittal, coronal, and transverse planes during stance phase for all specimens. Significant omnibus differences between mean joint angles are depicted by tick marks along the x-axis. Right column) Pairwise differences between each malalignment and N alignment. Significance occurs when zero lies outside the 95% confidence interval. Calcaneocuboid joint kinematics reflect motion of the cuboid with respect to the calcaneus.

http://dx.doi.org/10.2106/jbjs.18.00867

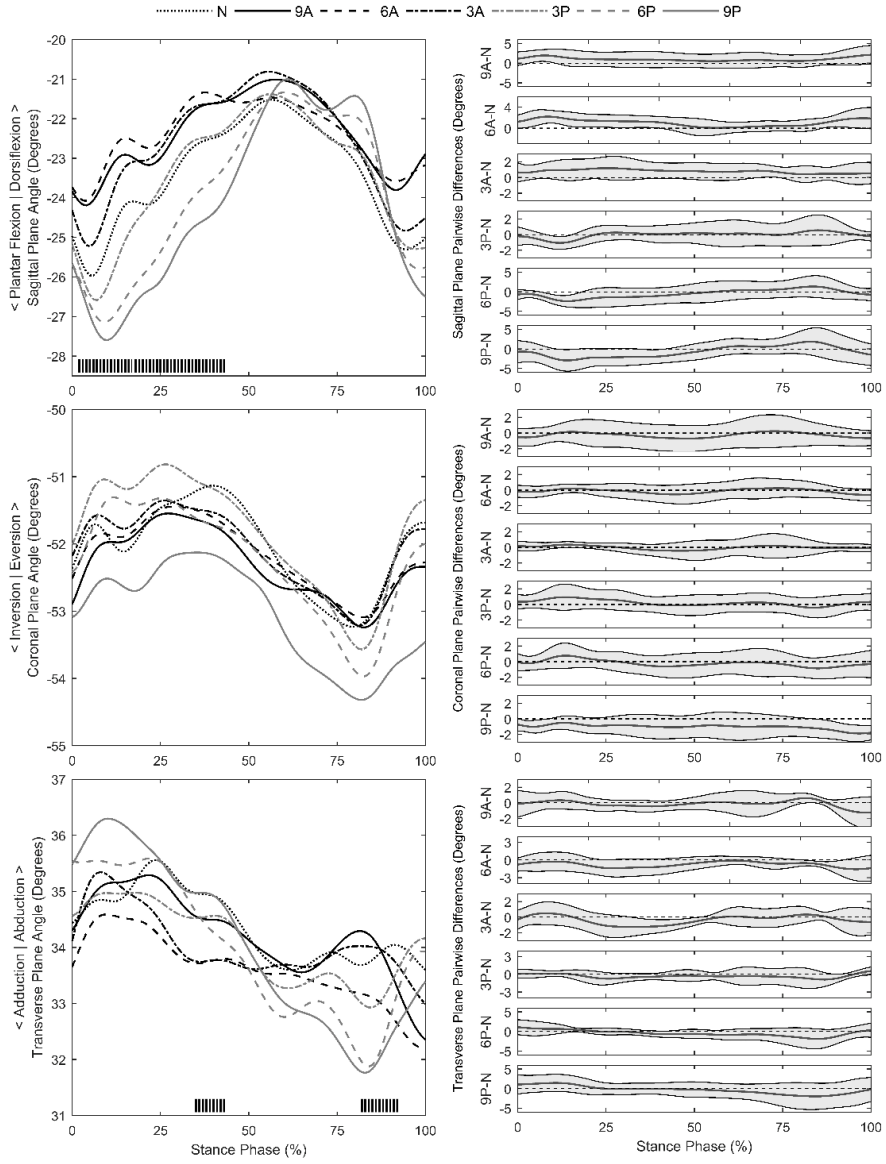

Figure C4: Left column) Mean naviculocuneiform joint kinematics in the sagittal, coronal, and transverse planes during stance phase for all specimens. Significant omnibus differences between mean joint angles are depicted by tick marks along the x-axis. Right column) Pairwise differences between each malalignment and N alignment. Significance occurs when zero lies outside the 95% confidence interval. Naviculocuneiform joint kinematics reflect motion of the medial cuneiform with respect to the navicular.

http://dx.doi.org/10.2106/jbjs.18.00867

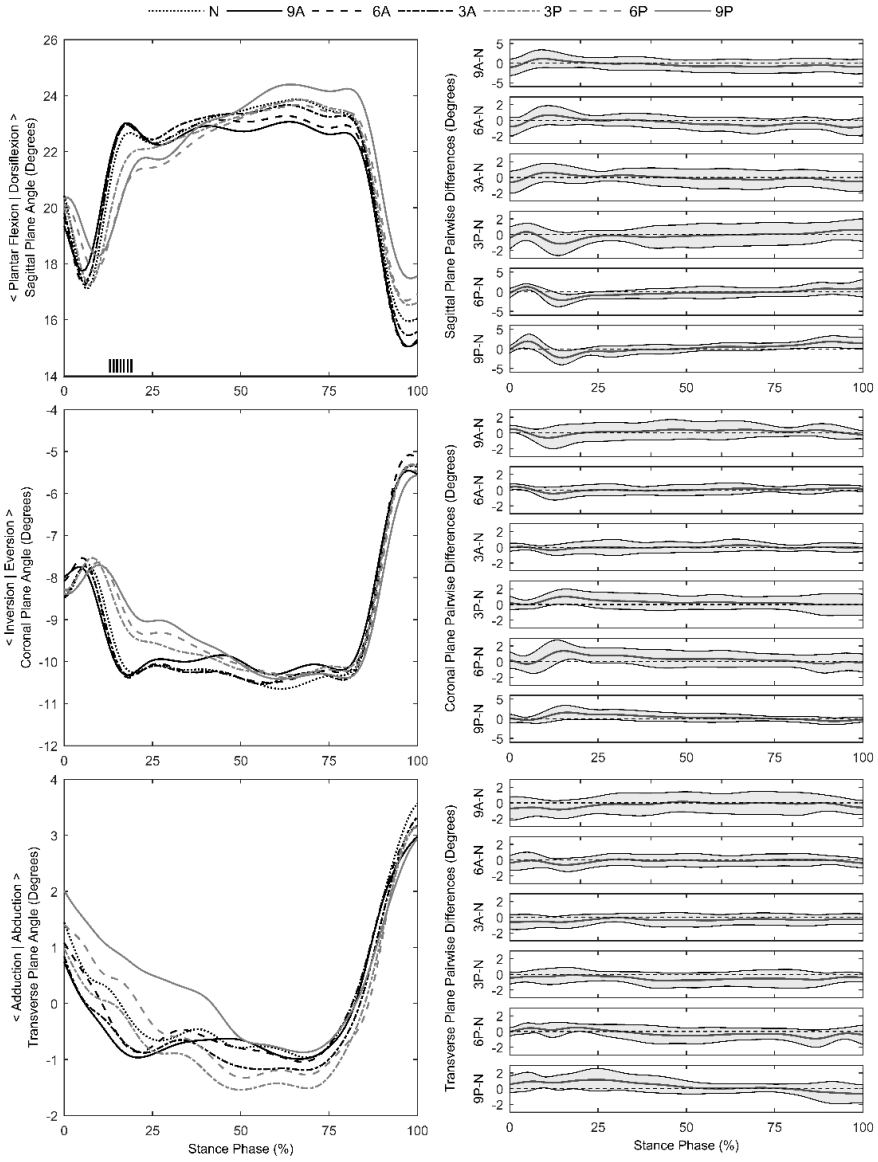

Figure C5: Left column) Mean first metatarsophalangeal joint kinematics in the sagittal, coronal, and transverse planes during stance phase for all specimens. Significant omnibus differences between mean joint angles are depicted by tick marks along the x-axis. Right column) Pairwise differences between each malalignment and N alignment. Significance occurs when zero lies outside the 95% confidence interval. First metatarsophalangeal joint kinematics reflect motion of the first proximal phalanx with respect to the first metatarsal.

http://dx.doi.org/10.2106/jbjs.18.00867

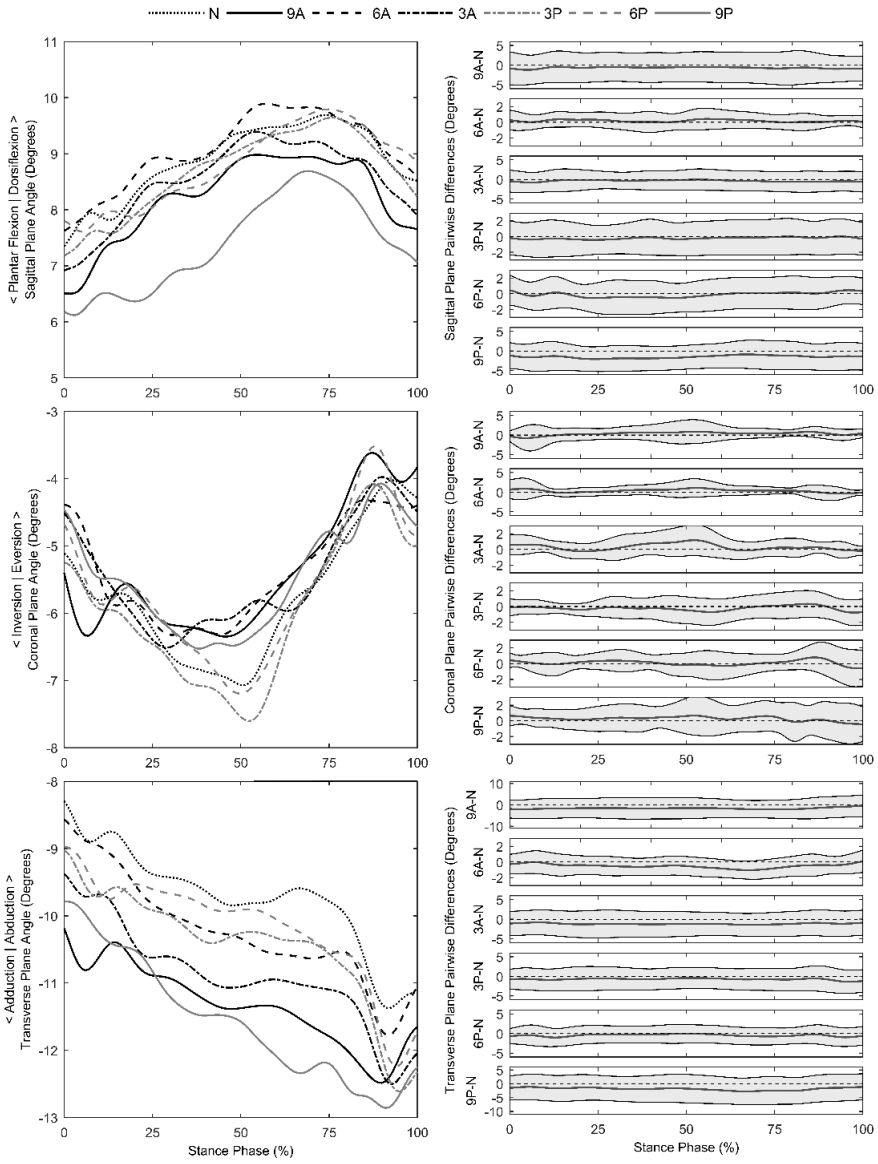

Figure C6: Left column) Mean first tarsometatarsal joint kinematics in the sagittal, coronal, and transverse planes during stance phase for all specimens. Significant omnibus differences between mean joint angles are depicted by tick marks along the x-axis. Right column) Pairwise differences between each malalignment and N alignment. Significance occurs when zero lies outside the 95% confidence interval. First tarsometatarsal joint kinematics reflect motion of the first metatarsal with respect to the medial cuneiform.

http://dx.doi.org/10.2106/jbjs.18.00867

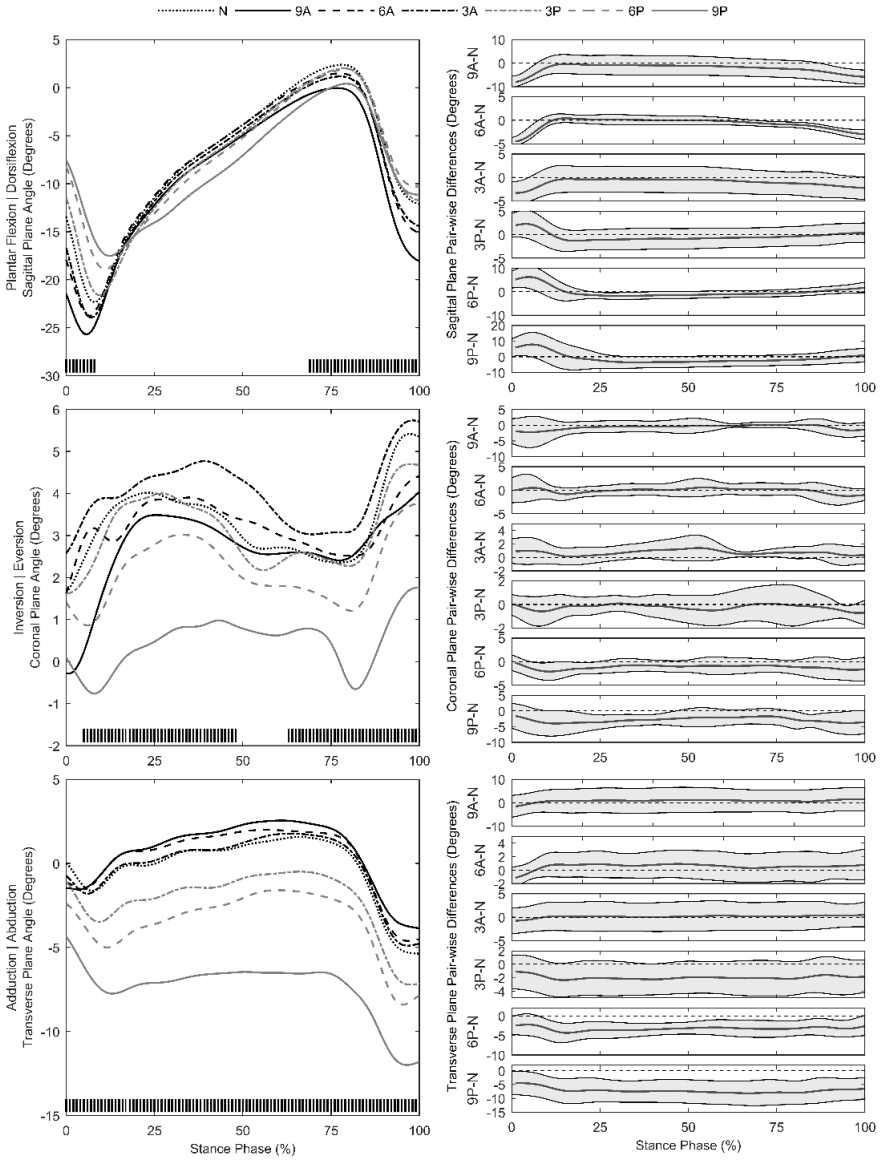

Figure C7: Left column) Mean first metatarsal to tibia relationship kinematics in the sagittal, coronal, and transverse planes during stance phase for all specimens. Significant omnibus differences between mean joint angles are depicted by tick marks along the x-axis. Right column) Pairwise differences between each malalignment and N alignment. Significance occurs when zero lies outside the 95% confidence interval. First metatarsal to tibia relationship kinematics reflect motion of the first metatarsal with respect to the tibia.

http://dx.doi.org/10.2106/jbjs.18.00867

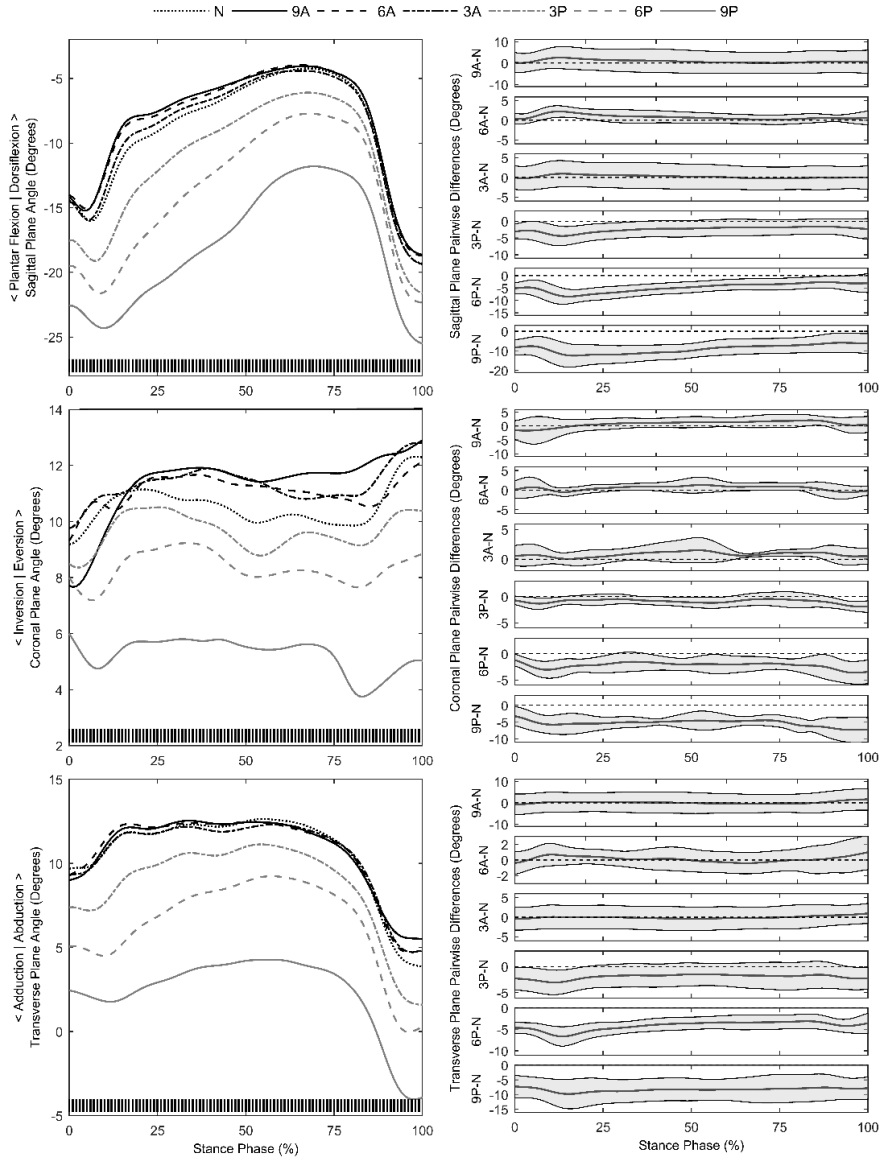

Figure C8: Left column) Mean first metatarsal to talus relationship kinematics in the sagittal, coronal, and transverse planes during stance phase for all specimens. Significant omnibus differences between mean joint angles are depicted by tick marks along the x-axis. Right column) Pairwise differences between each malalignment and N alignment. Significance occurs when zero lies outside the 95% confidence interval. First metatarsal to talus relationship kinematics reflect motion of the first metatarsal with respect to the talus.

http://dx.doi.org/10.2106/jbjs.18.00867

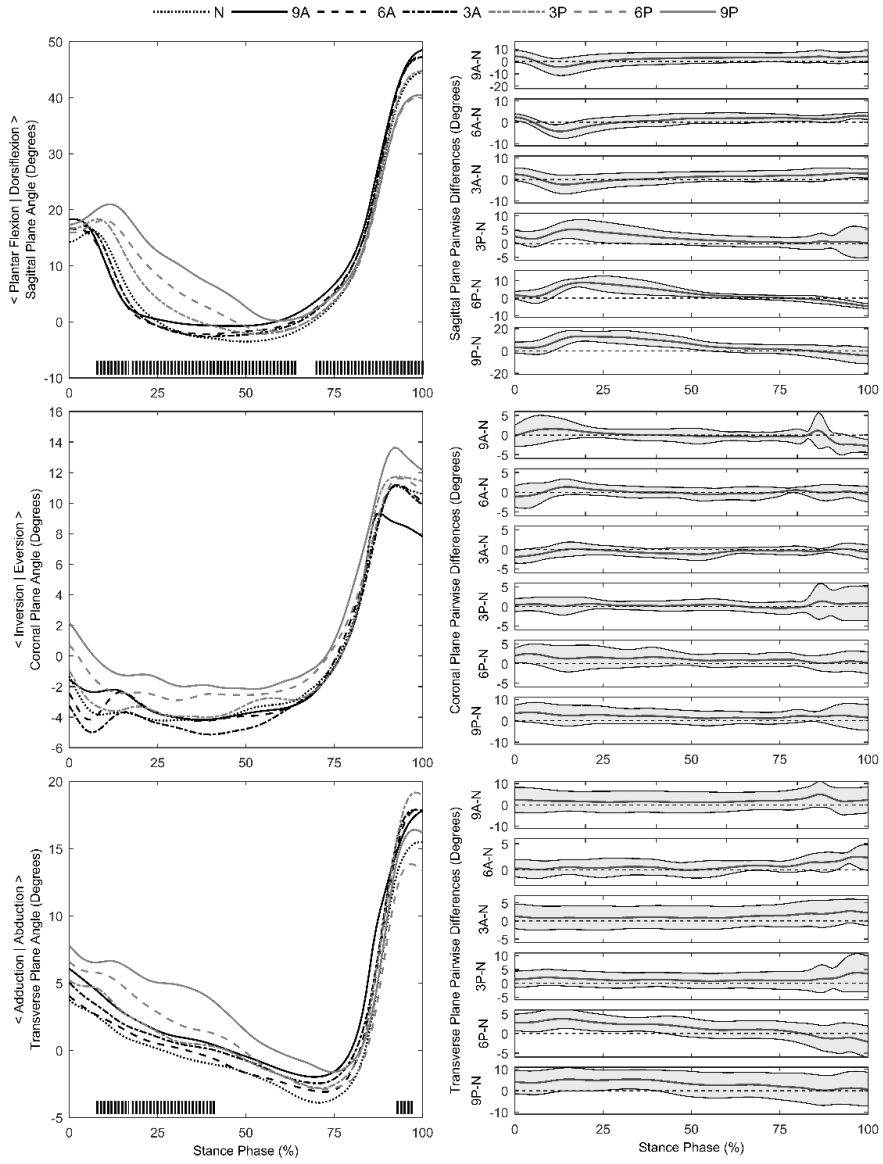

Figure C9: Left column) Mean fifth tarsometatarsal joint kinematics in the sagittal, coronal, and transverse planes during stance phase for all specimens. Significant omnibus differences between mean joint angles are depicted by tick marks along the x-axis. Right column) Pairwise differences between each malalignment and N alignment. Significance occurs when zero lies outside the 95% confidence interval. Fifth tarsometatarsal joint kinematics reflect motion of the fifth metatarsal with respect to the cuboid.

http://dx.doi.org/10.2106/jbjs.18.00867

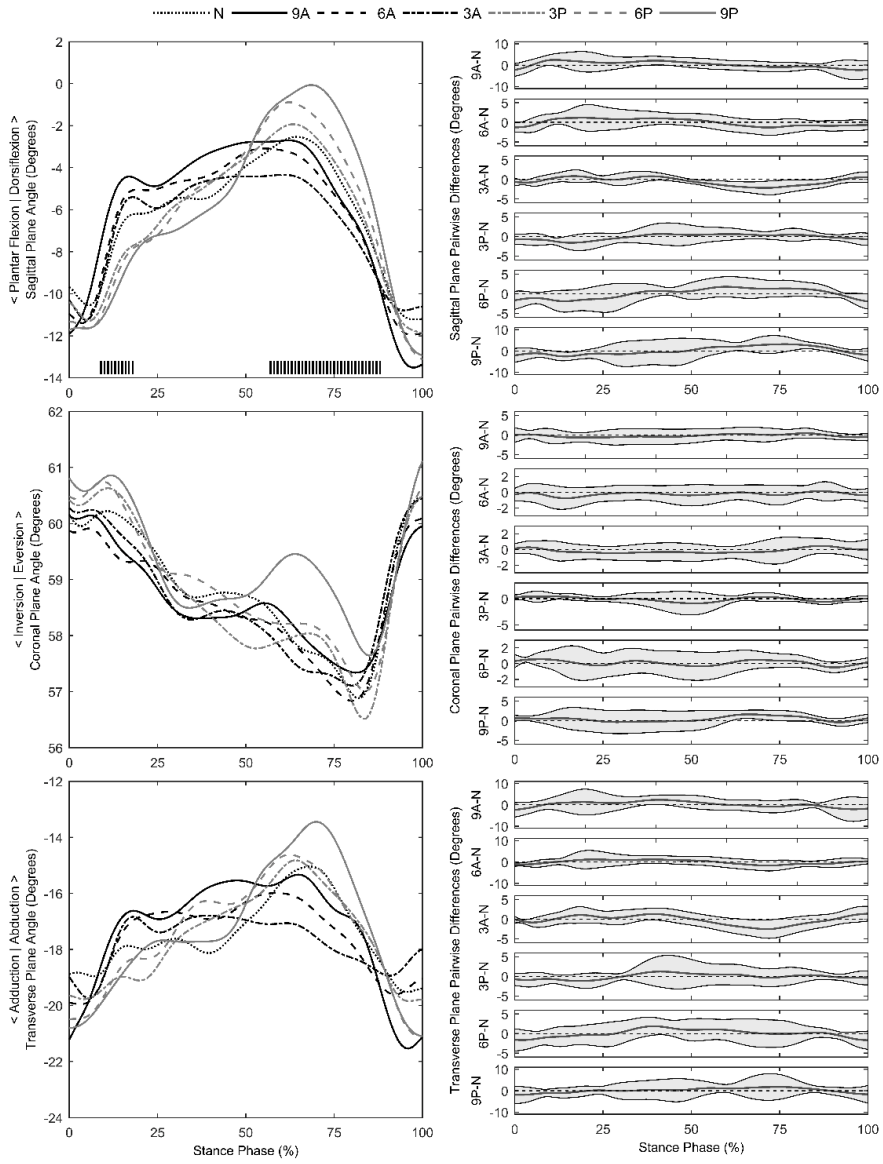

Figure C10: Left column) Mean talonavicular joint kinematics in the sagittal, coronal, and transverse planes during stance phase for all specimens. Significant omnibus differences between mean joint angles are depicted by tick marks along the x-axis. Right column) Pairwise differences between each malalignment and N alignment. Significance occur when zero lies outside the 95% confidence interval. Talonavicular joint kinematics reflect motion of the navicular with respect to the talus.